International Journal of Engineering & Technology, 7 (3.11) (2018) 218-222

International Journal of Engineering & Technology

Website: www.sciencepubco.com/index.php/IJET

Research paper

Magnesium-Impregnated Biochar for the Removal of Total Phosphorous from Artificial Human Urine

Nurul Fariha Mohd Idrus[1], Nurul´ Ain Jamion[2], Qistina Omar[3], Sheikh Ahmad Izaddin Sheikh Md Ghazali[2], Zaiton Abdul Majid[4], Soon Kong Yong[1]*

[1]*Faculty of Applied Sciences, Universiti Teknologi MARA, 40450 Shah Alam, Selangor, Malaysia*
[2]*Faculty of Applied Sciences, Universiti Teknologi MARA, 72000 Kuala Pilah, Negeri Sembilan, Malaysia*
[3]*Center of Foundation Studies, Universiti Teknologi MARA, 43800 Dengkil, Selangor, Malaysia*
[4]*Faculty of Science, Universiti Teknologi Malaysia, 81310 UTM Johor Bahru, Johor, Malaysia*
**Corresponding author E-mail: yongsk@salam.uitm.edu.my*

Abstract

Biochar has an alkaline and porous structure that could be a potential material for recycling phosphorous (P) from urine. Sawdust (SD) was pyrolyzed to produce sawdust biochar (SDB), and then impregnated with magnesium (Mg) to produce Mg-impregnated biochar (SDBM). Artificial human urine (AHU) solution was used for a batch sorption study, and various sorption parameters (i.e., sorbent/solution ratio, pH of AHU, and initial total P concentration of AHU) were optimized. The concentration of total P was measured using an inductively coupled plasma-optical emission spectroscopy (ICP-OES). The surface morphology and elemental analysis for SDB, SDBM and the struvite-loaded SDBM (SMSDB) were investigated using scanning electron spectroscopy-energy dispersive x-ray spectroscopy (SEM-EDX). The total P sorption capacity for SDBM (32755 mg/g) was higher than that of SDB (7782 mg/g) and SD (10682 mg/g). The optimum total P removal for SDBM (21.2%) was achieved at a sorbent/solution ratio of 0.06g/L at pH 9. Sorption of total P may have occurred on the heterogeneous surface of SDBM. The presence of struvite crystals indicates that phosphate was adsorbed and then precipitated on the surface of SDBM.

Keywords: *Carbon; heavy metals; immobilization; phosphate fertilizer; pyrolysis.*

1. Introduction

Phosphorous (P) is an important but finite resource, especially for the agricultural sector [1]. Sewage wastewater may contain high levels of P (e.g., phosphate and hydrogenphosphate) and nitrogen (N) compounds (e.g., ammonia and nitrate). However, seepage of untreated sewage wastewater to the environment may cause euthrophication to the water bodies. Hence, a continous removal of such compounds is required to ensure safe use of natural water resources. The N and P elements may be recovered from human and animal excreta (e.g, urine and manure). For example, crystallization process on swine wastewater converts soluble N and P compounds to form struvite [2], and then reused as a fertilizer [3], or as an immobilizing agent for heavy metals in soil [4]. However, practical use of struvite crystals is still limited due to its high solubility at acidic condition and high temperature [5].

Biomass is cheap materials from agricultural by-products and is suitable as feedstock for the production of sorbents. The pyrolysis process of hardwood biomass such as sawdust (SD) at high temperature (i.e., >500°C) produces a carbon-rich, chemically stable sawdust biochar (SDB) that may be suitable for recovery of nutrients (e.g., ammonia-N) from wastewater [6]. To further enhance the sorptive performance, post treatment on biochar has been conducted [7]. The ability of SDB for recovering P from aqueous phase may be increased by impregnating Mg ions on its surface [8]. However, the feasibility of the Mg-impregnation on SDB, and its effectiveness in removing P from human urine has not been thoroughly investigated.

This study aimed to synthesize SDB, and then impregnate it with Mg solution to produce Mg-impregnated sawdust biochar (SDBM) for batch sorption study of total P from artificial human urine (AHU). The objectives of this study were to optimize the sorption parameters (i.e., sorbent/solution ratio, pH of AHU, and initial P concentration of AHU), and to determine the mechanism of total P removal using sorption isotherm study. The Mg-impregnated sawdust biochar (SMSDB) was further characterized using SEM-EDX to elucidate the mechanism of total P removal by SDBM from AHU.

2. Materials and Methods

2.1. Synthesis of SDBM

The SD was collected from Syarikat Intertrade Company at Leboh Tapah, Klang, Malaysia, and was immediately washed with tap water and oven-dried at 100°C for 24 hours. The SD was converted to SDB by a slow pyrolysis process at 500°C for 2 hours in a nitrogen environment furnace. The resulting SDB was rinsed thoroughly with deionized water to approximately pH 8. Concentrated Magnesium chloride solution was prepared by dissolving 200 g of $MgCl_2.6H_2O$ in 1.0 L of deionized water. The SDBM was produced from the impregnation process, whereby, 40 g of oven-dried SDB was mixed with 400 mL of the concentrated $MgCl_2$ solution for 4 hours at 600 rpm using a rotator (Biosan RS-60). Then, the mixture was left to stand overnight, filtered with Whatman-1, and oven-dried at 60°C for 24 hours. The dried SDBM was sieved to a

Copyright © 2018 Authors. This is an open access article distributed under the Creative Commons Attribution License, which permits unrestricted use, distribution, and reproduction in any medium, provided the original work is properly cited.

diameter between 300 and 500μm, and stored in a silica-filled desiccator.

2.3. Batch Sorption Experiments

Batch sorption experiments were conducted using AHU stock (total P concentration: 181.71 mg/L) and its diluted solutions (Table 1) [9]. To prepare AHU, 1.5 liters of distilled water was prepared, and 416 mM of urea was added. Then, it was mixed until all the crystals were dissolved. Next, 154 mM of sodium chloride, 48 mM ammonium chloride, 21.10 mM sodium sulfate, and 17.6mM of sodium phosphate were added and mixed until the solution became clear. The pH of the solution was checked using a pH meter, and was maintained at within the pH range of 6.0-6.5. The pH of AHU solution was adjusted with 1*N* hydrochloric acid (HCl) or 1*N* sodium hydroxide (NaOH). In order to ensure a close similarity of AHU to human urine, 100 mg of albumin and 4.0 g of creatinine were slowly mixed into the 2 L of the AHU solution. The stock AHU solution was stored in a plastic container and refrigerated at around 4°C. The AHU stock was heated to a room temperature of 25°C before being used.

Table 1: Properties and composition of Artificial Human Urine (AHU) [9]

Property and Composition	Amount
pH	6 - 6.5
Specific gravity (g/ml)	1.020
Osmolality (mOsm/kg)	861
Urea (mM)	416
NaH_2PO_4 (mM)	17.60
NaCl (mM)	154.00
NH_4Cl (mM)	48.00
Na_2SO_4 (mM)	21.10

Sorption capacities (mg/g) for SD, SDB and SDBM were compared at a similar initial total P concentration (i.e., 181.71 mg/L); AHU pH 9; three days of contact time; temperature at 25°C at 0.06g/L of sorbent/solution ratio.

For the optimization of sorbent/solution ratio, SDBM was agitated with 30 mL of AHU (total P concentration: 181.71 mg/L) at various sorbent/solution ratios (i.e., 0.03, 0.06, 0.09, 0.12, 0.15g/L) at room temperature (i.e., 25°C) for four hours. The removal of total P as a function of pH of AHU was studied by agitating AHU stock at various pH values (i.e., 8, 9, 10, and 11) with SDBM at 0.06 g/L at room temperature (25°C) for four hours. For the sorption isotherm study, SDBM was agitated with AHU at pH 9, 0.06g/L, and 25°C for four hours at various initial total P concentrations (i.e., 30, 50, 70, 100, 200, and 800 mg/L). All mixtures of SMDB and AHU were kept for three and 30 days at 25°C, after which the residual AHU solutions were filtered through the Whatman 1 filter paper, and the concentration for total P was analyzed using ICP-OES. All analyses were conducted in triplicates. The percentage removal for total P (%) and equilibrium sorption capacity for total P, q_e (mg/g) were determined with equations (1) and (2), respectively.

$$\text{Percentage removal for Total P (\%)} = (C_o - C_e)/C_o \times 100 \quad (1)$$

$$q_e = V(C_o - C_e)/m \quad (2)$$

Sorption data were studied with the non-linear Langmuir (3) and Freundlich isotherm models (4), using the non-linear plotting software (i.e., SigmaPlot 12):

$$q_e = \frac{Q_{max} \cdot K_L \cdot C_e}{1 + K_L \cdot C_e} \quad (3)$$

$$q_e = K_F \cdot C_e^{1/nF} \quad (4)$$

where C_o and C_e (mg L^{-1}) are the initial and equilibrium concentrations for Total P, respectively; V is the volume of AHU solution (L); m is the mass of SDBM (g); K_L (L mg^{-1}) is the equilibrium constant for Langmuir model; K_f is the Freundlich constant that is related to sorption capacity of total P; and n (L mg^{-1}) is the Freundlich constants that is related to sorption intensity [10].

2.2. Physico-Chemical Characterization

The SD, SDBM and SMSB samples were sieved to 0.2 mm particle diameter and were dried thoroughly prior to characterization. Proximate analyses were conducted on SD using thermo gravimetric analysis (TGA) at a heating rate of 10°C/min and a peak temperature of 900°C in nitrogen atmosphere.

The surface morphology and surface elemental composition for SD, SDB, SDBM, and SDBMS were analyzed using scanning electron microscopy and energy dispersive x-ray spectroscopy, respectively (SEM-EDX) (Hitachi TM3030plus). All uncoated samples were mounted on a copper stub using a double-stick carbon tape. The elemental distribution for SDBM and SDBMS was mapped on SEM images to study the association of elements and to identify the compounds on the surface of SDBM and SDBMS.

3. Results and Discussion

3.1. Total P Sorption Capacities for SD, SDB and SDBM

Total P sorption capacity for SD, SDB, and SDBM were shown in Fig.

1. Total P sorption capacity for SDB (i.e. 7782 mg/g) was lower than SD (i.e., 10682 mg/g). Pyrolysis at high temperatures (i.e., 500°C) may have decreased the ability of biochar to grasp on cationic nutrients [11]. The amount of oxygen-containing functional groups (i.e., hydroxyl, carboxyl, carbonyl, and ether) were lost from the surface possibly due to the dehydration and physical core degradation during the pyrolysis process on SD [12]. However, the impregnation of Mg(II) ions had increased the total P sorption capacity (i.e., 10682 mg/g) for SDBM. The presence of positive-charged Mg(II) ions may have enhanced the attraction for the negative-charged P anions (i.e., phosphate, or hydrogenphosphate) on to the surface of SDBM [13]. Moreover, the presence of ammonium ion in AHU may have formed struvite crystals on the surface of the SDBM.

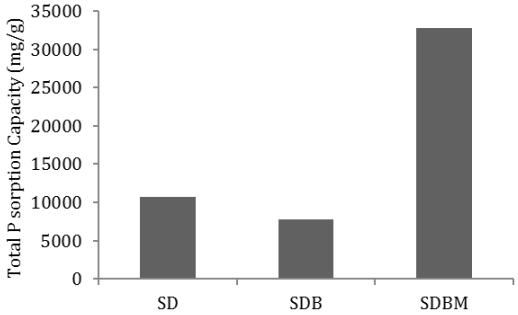


Fig. 1: Total P sorption capacity (mg/g) for SD, SDB, and SDBM (Initial Total P concentration: 181.71 mg/L; pH 9; contact time: three days; temperature 25°C)

3.2. Effect of SDB Dosage

The effects of the sorbent/solution ratio on Total P removal (%) from AHU by SDBM were shown in Fig. 2. Sorption of total P was rapidly increased from the 0.03g/L (7.6%), reaching a plateau at 0.06g/L (21.2%), and then slightly decreased until 0.15g/L (17.3%). Therefore, all of the sorption experiment will adopt the optimal sorption dosage (i.e., 0.06g/L) for all of the remaining parameters.

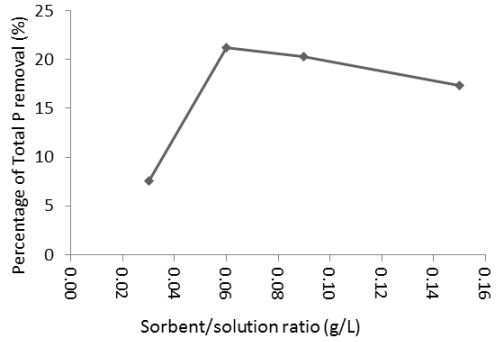


Fig. 2: Percentage of total P removal (%) as a function of SDBM sorbent/solution ratio (Initial total P concentration: 181.71 mg/L; pH 9; contact time: three days; temperature 25°C)

3.3. Effect of Initial Ahu Ph.

The effect of initial pH on the Total P removal (%) is shown in Fig. 3. Removal of total P was slightly increased from pH 8 (26.1%) to pH 9 (28.5%), then sharply decreased thereafter to 2.5% and 3.5% at pH 10 and 11, respectively. This finding corroborates with those from literature (i.e., pH 7.5 - 9.0) [14]. The increased in pH caused the decrease of concentrations for Mg(II) and ammonium ion in AHU, while increasing the concentration for phosphate ion [15]. At pH >9, Mg(II) ion may have precipitated to form Mg hydroxide, and the ammonium ions may have been deprotonated to form ammonia. These may lead to a decrease of available cations (i.e., Mg(II) and ammonium ions) that may also decrease the fixation of phosphorous in the aqueous phase, thereby, contributing to a lower percentage of removal for total P. Therefore, a further sorption experiment in this study was carried out at pH 9.

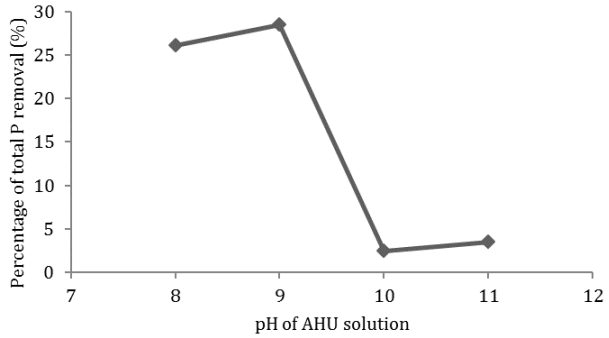


Fig. 3: Percentage of total P Removal (%) As A Function Of Ph Of AHU Solution (Initial Total P Concentration: 181.71 Mg/L; Sorbent/Solution Ratio: 0.06g/L; Agitation Time: Three days; temperature 25°C)

3.4. Total P Sorption Isotherm

Fig. 4 shows Total P sorption capacity for SDBM at 30 day-contact time, and various initial Total P concentrations (i.e., 30, 50, and 70 mg/L) of the AHU solution. Total P sorption capacity gradually increased from 7664 mg/g to 13835 mg/g at 70 mg/L. at 70 mg/L of total P in the urine. The recovery of phosphate as struvite is optimal when the concentration of phosphate is above 50 mg L^{-1} [16].

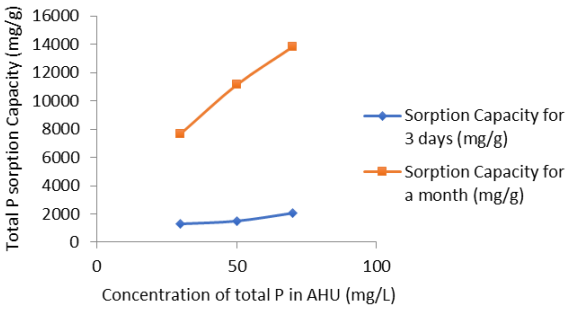


Fig. 4: Total P sorption capacity (mg/g) by SDBM as a function of initial total P concentration of AHU (mg/L) at three days and one month of contact time (Sorbent/solution ratio: 0.06g/L; solution pH 9; temperature 25°C)

Fig. 5 shows the total P sorption capacity for SDBM (q_e, mg/g) as a function of equilibrium concentration of total P (C_e, mg/L). The q_e value was steadily increased from 1295 mg/g to 5240 mg/g and further progress until it reached 6160 mg/g. The sorption of total P by SDBM is best described by the Freundlich model (R^2=0.968) compare to Langmuir model (R^2=0.909). The n value is 2.54, which indicates favorable nature of the sorption process [17]. The large K_f (604.7) and q_{max} values (e.g., 8026 mg/g) indicates greater sorption capacity of SDBM for total P [18].

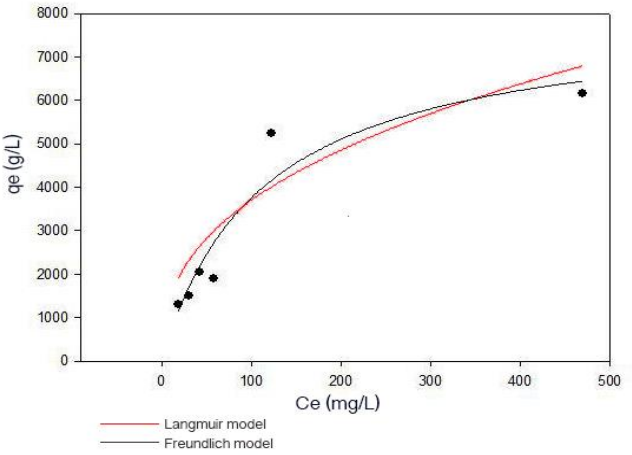


Fig. 5: Langmuir and Freundlich adsorption isotherm plots for total P sorption by SMSDB (Sorbent/solution ratio: 0.06g/L; solution pH: 9; contact time: three days; temperature 25°C)

3.4. Physico-Chemical Characterization

Multiple stages of thermal decomposition for SD are shown in Fig. 6. The first stage of SD thermal decomposition occurred at 164°C, whereby, a mass loss of difference of 6.0% was attributed to dehydration. The second stage consisted of two endothermic processes: (1) decomposition of hemicellulose at around 335°C, and (2) decomposition of cellulose at around 360°C [19]. The weight percentage of volatile matter was 42.6%. Compared to the decomposition for hemicellulose and cellulose, the rate of decomposition for lignin was relatively slower at a wider range of temperature (i.e., 150–900°C) [20]. The combined weight for fixed carbon and ash was 51.4%. The elemental compositions for SD, SDB and SDBM are shown in Table 2. Pyrolysis process increased the C/O ratio, indicating that the resulting SDB is chemically more stable than SD [21]. The content of Mg in SDBM was 2%.

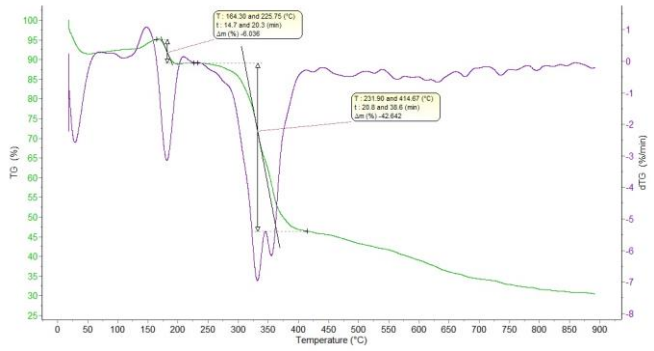


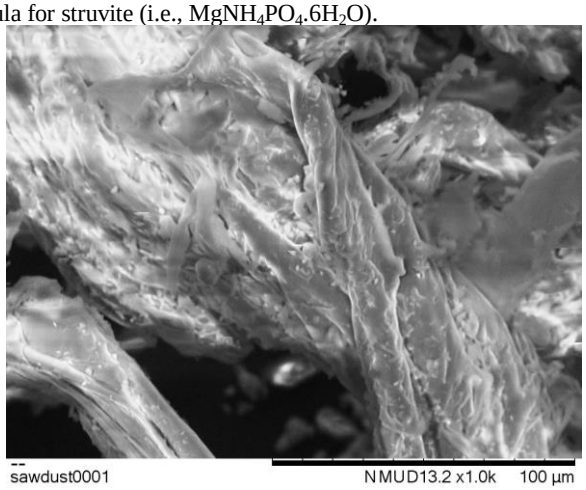
Fig. 6: Thermogram for SD

Table 2: Elemental composition for SD, SDB and SDBM

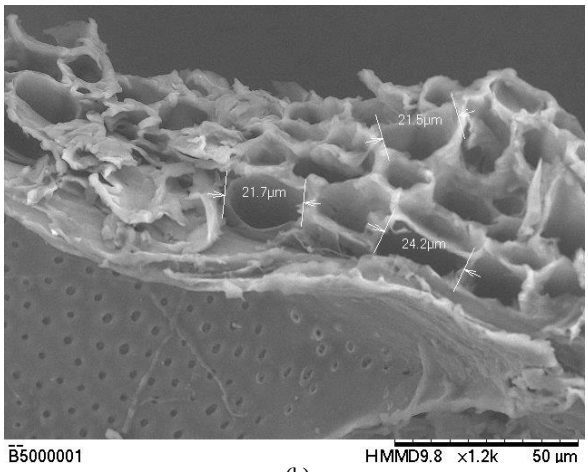
	SD	SDB	SDBM
C	48±2	71±9	67±1
O	47±2	19±4	22±1
Ca	5±3	1±1	4±1
Mg	0	0	2±0
S	0	0	0
N	0	2±4	0

Figures 7(a), (b), (c) and (d) show SEM images for SD, SDB, SDBM and SMSDB, respectively. The surface of SD (Fig. 7(a)) was rough and compact with no pores on its surface. For SDB (Fig. 7b), the pyrolysis process had formed a porous structure on its surface. The process of impregnating Mg(II) ions did not cause any apparent changes on the surface of SDBM (Fig. 7(c)).

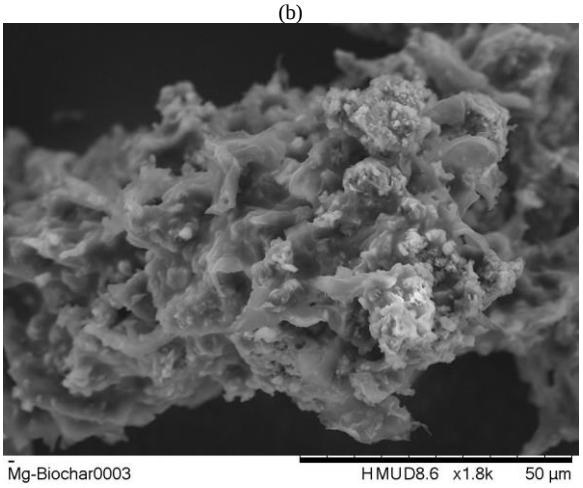
Table 2 shows the composition of elements for SD, SDB and SDBM. Overall, all samples primarily consisted of C and O, with negligible content of Ca, N and S. Pyrolysis process increased the C content from 48±2% in SD to 71±9% in SDB. The content of O had decreased to 19±4% after the pyrolysis process. This may have attributed to the decrease of oxygen-containing functional group in SDB. The impregnation process only managed to increase 2±0% of Mg in SDBM. The presence of Mg on the surface and the pores of SDBM was indicated by the blue Mg map in Fig. 8(a). Fig. 7(d) shows a coffin, prismatic crystal on the surface of SDBMS, which is consistent with the shape of a struvite [22]. The element maps for SDBMS are shown in Fig. 8b. The chemical composition of the crystal primarily consisted of Mg, N, P and O, and these elements are strongly associated with the chemical formula for struvite (i.e., $MgNH_4PO_4.6H_2O$).



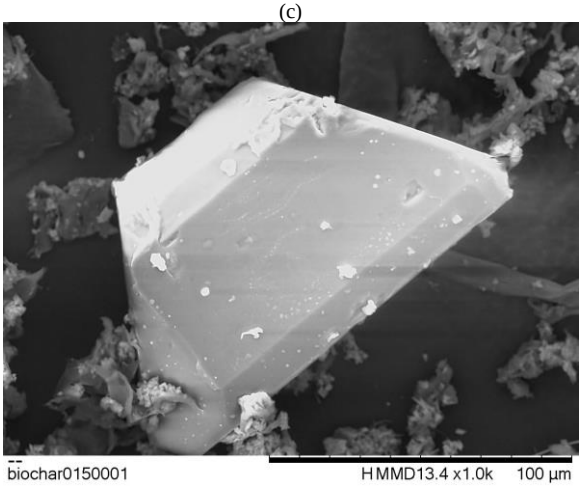
(a)



(b)



(c)



(d)

Fig. 7: SEM images for (a) SD, (b) SDB, (c) SDBM, and (d) struvite crystal on the surface of SDBMS

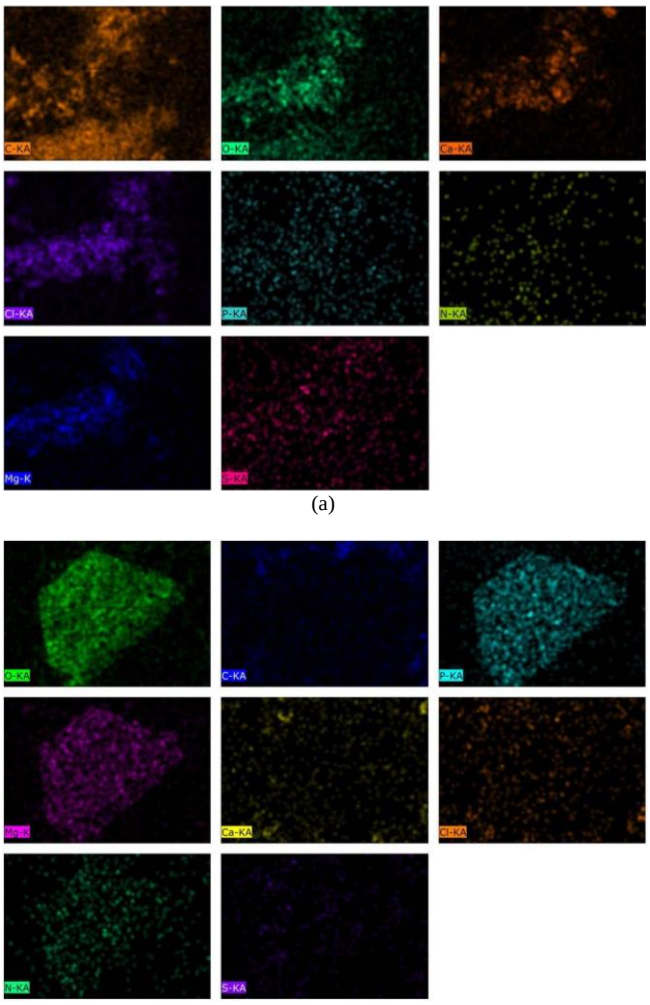


Fig. 8: EDX map of elements for (a) SDBM, and (b) struvite crystal on the surface of SMSDB

4. Conclusion

This study had successfully synthesized SDBM and removed total P from AHU. Total P sorption capacity for SDBM was higher compared to SDB and SD. Pyrolysis process slightly decreased the sorption capacity of SDB for total P, but impregnation of Mg had increased the total P sorption capacity for SDBM. Even with a low content of Mg in SDBM (i.e., 2%), struvite had been successfully precipitated on the surface of SDBM from AHU solution, and with a total P q_{max} value of 8026 mg/g. The resulting SDBMS may be used as a slow-release fertilizer. Further analysis such as desorption kinetics of total P was required to further understands the slow-release kinetics of total P from SDBMS. Other key physical characteristics such as distribution of pore sizes and pore volume may also influence struvite precipitation. Hence, further investigation is warranted to enhance the loading capacity of struvite in SDBM.

Acknowledgement

The authors gratefully acknowledge the financial support from the Ministry of Higher Education, Malaysia (FRGS/1/2017/WAB05/UITM/03/2) and Universiti Teknologi MARA (UiTM) for providing the use and analysis of SEM-EDX.

References

[1] E. Desmidt, K. Ghyselbrecht, Y. Zhang, et al., Global phosphorus scarcity and full-scale P-recovery techniques: a review. Critical Reviews in Environmental Science and Technology 45 (2015) 336-384.

[2] B. Kim, W. Lee, H. Lee & J. Rim, Ammonium nitrogen removal from slurry-type swine wastewater by pretreatment using struvite crystallization for nitrogen control of anaerobic digestion. Water Science and Technology 49 (2004) 215-222.

[3] J.L. Kovar & G.M. Pierzynski, Methods of phosphorus analysis for soils, sediments, residuals, and waters second edition. Southern Cooperative Series Bulletin 408 (2009).

[4] Q.Y. Ma, T.J. Logan & S.J. Traina, Lead immobilization from aqueous solutions and contaminated soils using phosphate rocks. Environmental Science & Technology 29 (1995) 1118-1126.

[5] E. Ariyanto, H.M. Ang & T. Sen, Effect of initial solution pH on solubility and morphology of struvite crystals. Chemeca 2011: Engineering a Better World: Sydney Hilton Hotel, NSW, Australia, 18-21 September 2011 (2011) 1706.

[6] S.F. Halim, S.K. Yong & C.C. Tay, Ammonia Nitrogen Adsorption using Spent Mushroom Substrate Biochar (SMSB). Pertanika Journal of Science and Technology 25 (2017) 9-20.

[7] T. Sizmur, T. Fresno, G. Akgül, H. Frost & E. Moreno-Jiménez, (2017), Biochar modification to enhance sorption of inorganics from water. pp.

[8] C. Fang, T. Zhang, P. Li, R.F. Jiang & Y.C. Wang, Application of magnesium modified corn biochar for phosphorus removal and recovery from swine wastewater. International Journal of Environmental Research and Public Health 11 (2014) 9217-9237.

[9] S. Chutipongtanate & V. Thongboonkerd, Systematic comparisons of artificial urine formulas for in vitro cellular study. Analytical Biochemistry 402 (2010) 110-112.

[10] M.A. Zazouli, D. Balarak, Y. Mahdavi & M. Ebrahimi, Adsorption rate of 198 reactive red dye from aqueous solutions by using activated red mud. Iranian Journal of Health Sciences 1 (2013) 36-43.

[11] N. Zhou, H.G. Chen, J.T. Xi, et al., Biochars with excellent Pb (II) adsorption property produced from fresh and dehydrated banana peels via hydrothermal carbonization. Bioresource technology 232 (2017) 204-210.

[12] M.J. Antal & M. Grønli, The art, science, and technology of charcoal production. Industrial & Engineering Chemistry Research 42 (2003) 1619-1640.

[13] C. Takaya, L. Fletcher, S. Singh, U. Okwuosa & A. Ross, Recovery of phosphate with chemically modified biochars. Journal of Environmental Chemical Engineering 4 (2016) 1156-1165.

[14] X.D. Hao, C.C. Wang, L. Lan & M.C.M. Van Loosdrecht, Struvite formation, analytical methods and effects of pH and Ca^{2+}. Water Science and Technology 58 (2008) 1687-1692.

[15] A. Miles & T.G. Ellis, Struvite precipitation potential for nutrient recovery from anaerobically treated wastes. Water Science and Technology 43 (2001) 259-266.

[16] W. Moerman, J. de Danschutter, B. de Ru, et al., In-line phosphate recovery as nuisance control for struvite clogging sensitive wastewater or sludges. IWA Nutrient Removal and Recovery (2012) 23-25.

[17] V.S. Munagapati & D.-S. Kim, Equilibrium isotherms, kinetics, and thermodynamics studies for congo red adsorption using calcium alginate beads impregnated with nano-goethite. Ecotoxicology and Environmental Safety 141 (2017) 226-234.

[18] M.G. Ismail, C.N. Weng, H.A. Rahman & N.A. Zakaria, Freundlich Isotherm Equilibrium Equastions in Determining Effectiveness a Low Cost Absorbent to Heavy Metal Removal In Wastewater (Leachate) At Teluk Kitang Landfill, Pengkalan Chepa, Kelantan, Malaysia. Journal of Geography and Earth Science 1 (2013) 1-8.

[19] P. Llorach-Massana, E. Lopez-Capel, J. Peña, et al., Technical feasibility and carbon footprint of biochar co-production with tomato plant residue. Waste Management 67 (2017) 121-130.

[20] A. Zabaniotou, O. Ioannidou, E. Antonakou & A. Lappas, Experimental study of pyrolysis for potential energy, hydrogen and carbon material production from lignocellulosic biomass. International Journal of Hydrogen Energy 33 (2008) 2433-2444.

[21] C.A. Mullen, A.A. Boateng, N.M. Goldberg, et al., Bio-oil and biochar production from corn cobs and stover by fast pyrolysis. Biomass and bioenergy 34 (2010) 67-74.

[22] C.K. Chauhan & M.J. Joshi, In vitro crystallization, characterization and growth-inhibition study of urinary type struvite crystals. Journal of Crystal Growth 362 (2013) 330-337.